Superfluid vortex reconnections at non-zero temperatures - TBD

P. Z. Stasiak, C.F. Barenghi, and A. Baggaley
School of Mathematics, Statistics and Physics, Newcastle University, Newcastle upon Tyne, NE1 7RU, United Kingdom

Y. Xin, Y. Alihosseini, and W. Guo
Department of Mechanical Engineering, FAMU-FSU College of Engineering, Florida State University, Tallahassee, Florida 32310, USA

L. Galantucci
Istituto per le Applicazioni del Calcolo "M. Picone" IAC CNR, Via dei Taurini 19, 00185 Roma, Italy

G. Krstulovic
Université Côte d'Azur, Observatoire de la Côte d'Azur, CNRS,Laboratoire Lagrangre, Boulevard de l'Observatoire CS 34229 - F 06304 NICE Cedex 4, France

(Dated: October 30, 2024)

The minimum separation between reconnecting vortices in fluids and superfluids obeys a universal scaling law with respect to time. The pre-reconnection and the post-reconnection prefactors of this scaling law are different, a property related to irreversibility. Using experiments and a numeric model which fully accounts for the independent dynamics of the superfluid vortex lines and the thermal normal fluid component, we determine the temperature dependence of these prefactors. We also numerically show that each vortex reconnection event represents a sudden injection of energy in the normal fluid. Finally we argue that in a turbulent flow, these punctuated energy injections can sustain the normal fluid in a perturbed state, provided that the density of superfluid vortices is large enough.

Introduction.— Reconnections are the fundamental events that change the topology of the field lines in fluids and plasmas during their time evolution. Reconnections thus determine important physical properties, such as mixing and inter-scale energy transfer in fluids [1], or solar flares and tokamak instabilities in plasmas [2]. The nature of reconnections is more clearly studied if the field lines are concentrated in well-separated filamentary structures: vortices in fluids and magnetic flux tubes in plasmas. In superfluid helium this concentration is extreme, providing an ideal context: superfluid vorticity is confined to vortex lines of atomic thickness (approximately $a_0 \approx 10^{-10}$ m); a further simplification is that, unlike what happens in ordinary fluids, the circulation of a superfluid vortex is constrained to the quantized value $\kappa = h/m = 9.97 \times 10^{-8}$ m^2/s, where m is the mass of one helium atom and h is Planck's constant.

It was in this superfluid context that it was theoretically and experimentally recognized [3–8] that reconnections share a universal property irrespective of the initial condition: the minimum distance between reconnecting vortices, $\delta^{\pm}$, scales with time, t, according to the form

$$\delta^{\pm}(t) = A^{\pm}(\kappa|t - t_0|)^{1/2}, \qquad (1)$$

where t_0 is the reconnection time, and the dimensionless prefactors A^- and A^+ refer respectively to before ($t < t_0$) and after ($t > t_0$) the reconnection. The same scaling law was then found for reconnections in ordinary viscous fluids [9]. In the case of a pure superfluid at temperature $T = 0$ K, theoretical work based on the Gross-Pitaevskii equation (GPE) has shown that $A^+ > A^-$, that is, after the reconnection, vortex lines move away from each others faster than in the initial approach; this result has been related to irreversibility [10, 11]. Indeed, a geometrical constraint imposes that a piece of vortex length needs to be "deleted" during the reconnection process. In the GP model, this loss is possible by the emission of a rarefaction pulse created immediately after the reconnection [6, 12] which removes some of the kinetic energy and momentum of the vortex configuration. This vortex energy loss depends on the ratio A^+/A^-, which in turns defines the approaching angle of collision between the vortices, together with other several geometrical quantities [7, 11].

The temporal asymmetry $A^+ > A^-$ can be thus interpreted as a non-trivial manifestation of irreversibility, as it originates from an ideal hydrodynamic process independent of the small-scale regularisation mechanism of the fluid. Indeed, in classical fluid vortex reconnections, although the definition of A^+ is more delicate as circulation is not necessarily conserved, the same asymmetry $A^+ > A^-$ was reported [9]. Instead of the generation of rarefaction pulses, like in the case of $T = 0$ superfluids, close to the reconnection, the classical fluid creates a series of thin secondary structures that can be then efficiently dissipated by viscous dissipation.

The case of superfluid helium is more intriguing. Most experiments are performed at temperatures $T > 1$ K, a

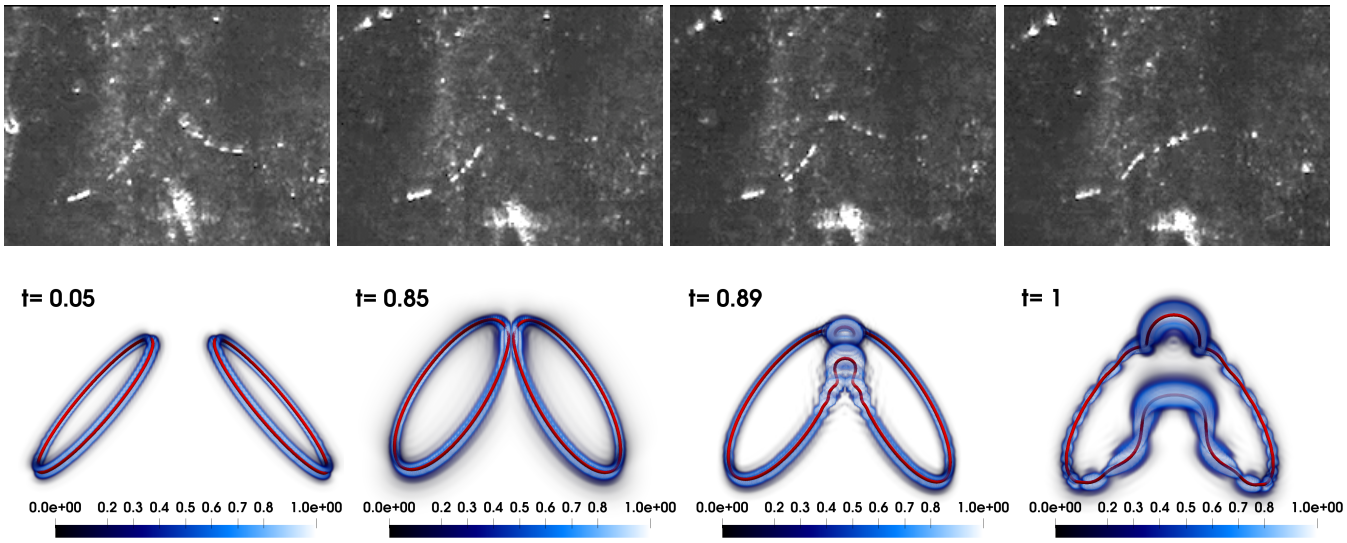

FIG. 1: *Top row:* Snapshots of experiments, details to be added here. If possible, improve quality of images *Bottom row:* Oblique collision of two circular vortex rings at different (dimensionless) times, here in units of $\tau = 0.183$s. The superfluid vortex lines are represented by red tubes (the radius has been greatly exaggerated for visual purposes); the scaled normal fluid enstrophy $\boldsymbol{\omega}^2/\boldsymbol{\omega}^2_{max}$ is represented by the blue volume rendering.

.

regime in which in addition to quantum vortices, thermal excitations constitute a viscous liquid called the *normal fluid*. The normal fluid can steal energy from filaments and dissipate it by viscous effects, opening in that way more routes towards irreversibility. Modern visualisation techniques rely on active tracer particles to decorate superfluid vortices [4, 13–15]. Numerous studies have provided insight into the post-reconnection dynamics and the prefactor A^+, but much less is known about A^- from experiments due to statistical likelihood of observation in the plane of view.

The aim of this Letter is to investigate the role played by the normal fluid in the reconnection dynamics. In particular, given the temperature dependence of the normal fluid's properties, we study experimentally and numerically the temperature dependence of the prefactors A^+ and A^- and numerically investigate the energy injected in the normal fluid. To achieve this aim we need a more powerful model than the GPE to account not only for the dynamics of the superfluid vortices, but also for the dynamics of the normal fluid. We show that at non-zero temperatures Eq. (1) and the relation $A^+ > A^-$ hold true, in agreement with experiments, revealing, for the first time, a temperature dependence of A^+/A^-. In addition, we show that a vortex reconnection represents an unusual kind of punctuated energy injection into the normal fluid which acts alongside the well-known (continual) friction. When applied to superfluid turbulence, this last result implies that, if the vortex line density (hence the frequency of reconnections) is large enough, vortex reconnections can maintain the normal fluid in a perturbed state.

Experimental Method.— **[Add details of the experimental method here.]** Note that GP simulations reported that particles trapped inside vortices do not drastically affect vortex reconnections [16]. Whereas in the particle-vortex system, vortex energy and momentum are also transferred to particles, these additional mechanisms do not modify the approaching rates. This argument was also supported by a scaling symmetry of the system which allows to draw conclusion for length-scales relevant to experiments.

Numerical Method.— We follow the approach of Schwarz [17] which exploits the vast separation of length scales between the vortex core a_0 and any other relevant distance, in particular the average distance between vortices, ℓ, in the case of turbulence. Vortex lines are described as space curves $\mathbf{s}(\xi, t)$ where ξ is arclength. The equation of motion of the vortex lines is

$$\dot{\mathbf{s}}(\xi,t) = \mathbf{v}_s + \frac{\beta}{(1+\beta)}\left[\mathbf{v}_{ns}\cdot\mathbf{s}'\right]\mathbf{s}' + \beta\mathbf{s}'\times\mathbf{v}_{ns} + \beta'\mathbf{s}'\times[\mathbf{s}'\times\mathbf{v}_{ns}]\,, \tag{2}$$

where $\dot{\mathbf{s}} = \partial\mathbf{s}/\partial t$, $\mathbf{s}' = \partial\mathbf{s}/\partial\xi$ is the unit tangent vector, $\mathbf{v}_n$ and $\mathbf{v}_s$ are the normal fluid and superfluid velocities at $\mathbf{s}$, $\mathbf{v}_{ns} = \mathbf{v}_n - \mathbf{v}_s$, and β, β' are temperature and Reynolds number dependent mutual friction coefficients [18]. The normal fluid velocity $\mathbf{v}_n$ is described as a classical fluid obeying the incompressible ($\nabla\cdot\mathbf{v}_n = 0$) Navier-Stokes equations:

$$\frac{\partial\mathbf{v}_n}{\partial t} + (\mathbf{v}_n\cdot\nabla)\mathbf{v}_n = -\frac{1}{\rho}\nabla p + \nu_n\nabla^2\mathbf{v}_n + \frac{\mathbf{F}_{ns}}{\rho_n}, \tag{3}$$

where $\mathbf{F}_{ns}$ is the mutual friction force that couples the normal fluid and the superfluid vortices, and acts

as an internal injection mechanism. In Eq. (3), $\rho = \rho_n + \rho_s$, where ρ_n and ρ_s are the normal fluid and superfluid densities, p is the pressure, and ν_n is the kinematic viscosity of the normal fluid. Equations (2) and (3) are solved in dimensionless form by rescaling them by the characteristic time τ and length λ. The algorithm for vortex reconnections is standard [19]. We consider two distinct initial vortex configurations at three temperatures $T = 0$ K, 1.9 K and 2.1 K corresponding to the superfluid fractions $\rho_s/\rho = 100\%$, 58% and 26%. To compare with experiments, the unit of length is set to $\lambda = 1.59 \times 10^{-4}$ m, and the time units to $\tau = 0.183$ s at $T = 0$ K and 1.9 K, and $\tau = 0.242$ s at $T = 2.1$ K, see also [20] for details. All configurations lead to a vortex reconnection. The first configuration consists of two vortex rings of (dimensionless) radius $R \approx 1$ in a tent-like shape which collide obliquely making an initial angle α with the vertical direction, as shown in Fig. 1, and, schematically, in Fig. 2b. By changing the parameter α, we create a sample of 12 realizations at each temperature (again, see the Supplementary Material [20] for details). The second configuration is the Hopf link, shown schematically in Fig. 2b. It consists of two perpendicular linked rings of radius $R \approx 1$ with an offset in the xy-plane. By changing the offset, we create a sample of 49 reconnections at each temperature, as described in the Supplementary Material (SM) [20]. In all cases, normal fluid structures generated by moving superfluid vortex rings [21], are initially prepared to eliminate the transient phases (see SM for details).

Scaling law. — In the experiment, two reconnections were observed where both A^+ and A^- could be identified and calculated, at $T = 1.65K$ and $T = 2K$, plotted as orange triangles in Fig. 2b. Their corresponding minimal distances are displayed in the inset. The pre-reconnection factor A^- lies within the 0.4-0.6 range, consistent with the results of the numerics, and a clear temperature effect between a superfluid component majority and normal fluid component majority. In the case of the Hopf link we have performed 147 simulations (49 across 3 temperatures) as shown in Fig. 2a and verified Eq. (1) for the minimum distance $\delta^\pm$. The prefactors $A^\pm$ have been computed in the shaded region of the figure. In the pre-reconnection regime ($t < t_0$) we observe a clear segregation of the values of A^- due to temperature: the minimum distance grows more rapidly with time if the temperature is lowered. In stark contrast, there is almost no memory of the temperature in the post-reconnection regime ($t > t_0$).

At $T = 0$ K, our calculations for superfluid helium (black symbols in Fig. 2b) are in good agreement with previous results obtained with the GPE [10] (green diamonds), showing irreversible dynamics. In addition, the computed values of $A^- \approx 0.4$-0.6 at $T = 0$ K are consistent with analytical calculations [22, 23]. At non-zero temperatures, our results confirm the irreversibility

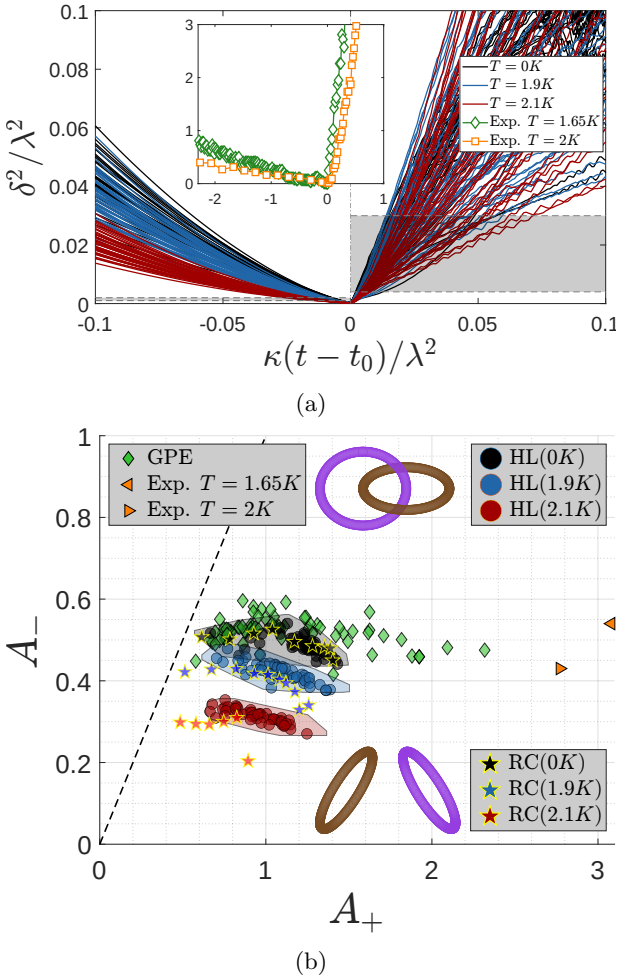

FIG. 2: *(a)*: Time evolution of the (dimensionless) minimum distance squared δ^2 plotted versus (dimensionless) $\kappa(t - t_0)$ for the Hopf link reconnections at $T = 0K, 1.9K$ and $2.1K$ (black, blue and red respectively). The grey shaded areas are the regions used to estimate the prefactors $A^\pm$. *Inset:* Experimental superfluid helium data. *(b)*: Comparison of all prefactors: Hopf links (*HL*, circles), ring collisions (*RC*, stars with yellow outline), GPE-data from Villois *et al.* [10] (green diamonds) and experimental results from this study (orange triangles). The shaded areas associated with each colour represent the convex hull of errors for each temperature. Schematic rendering of initial conditions are included.

of vortex reconnections observed at $T = 0$ as A^+ is always larger than A^-. Importantly, this asymmetry is recovered in all our simulations, regardless of their initial condition. The same asymmetry between A^+ and A^- at non-zero temperatures has been observed for reconnections in finite-temperature Bose-Einstein condensatates [24], although in this work the system is not homogeneous (the condensate is confined by

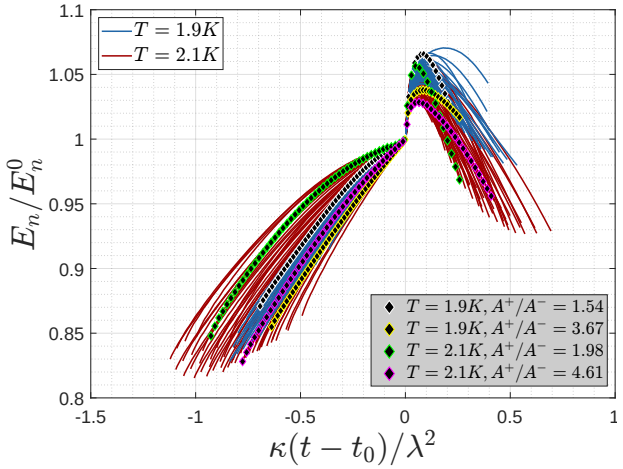

FIG. 3: Normal fluid kinetic energy E_n scaled by E_n^0 (the kinetic energy at $t = t_0$), plotted versus (dimensionless) $\kappa(t - t_0)$ for the Hopf link reconnections. Black diamonds represent the simulations with minimum and maximum prefactor ratios A^+/A^- at $T = 1.9$ K and $T = 2.1$ K respectively.

a harmonic trap) and the thermal component is a ballistc gas, not a viscous fluid. Note that the vortex reconnections in classical viscous fluids reported in [9] also display a clear 1/2 power-law scaling for the minimum distance with $A^- \approx 0.3$-0.4, which again shows good agreement with our results. The scaling law (Eq. 1) and the range of values of A^- hence appear to have a universal character in vortex reconnections, independently of the nature of the fluid, classical or quantum, and temperature.

Energy injection. — The normal fluid impacts the dynamics of reconnecting superfluid vortices via the temperature dependent mutual friction coefficients. Conversely, the motion of superfluid vortices involved in the reconnection process influence, significantly, the dynamics of the normal fluid. Figure 3 indeed shows that the normal fluid energy, E_n, suddenly increases at the reconnection time by an amount ($\approx 5\%$) which is smaller but comparable to the continuous energy increase as vortex lines approach each other. Indeed the curvature $\zeta = |\mathbf{s}''|$ of the vortex line spikes at $t = t_0$ when the reconnection cusp is created, and, in the first approximation [25], the magnitude of the energy injected in the normal fluid per unit time I is proportional to the strength of the mutual friction force $\mathbf{F}_{ns}$ which scales as $|\mathbf{F}_{ns}(\mathbf{s})| \propto |\dot{\mathbf{s}} - \mathbf{v}_n| \propto |\dot{\mathbf{s}}| \propto \zeta$. This sudden transfer of energy [26] from the superfluid vortex configuration to the normal fluid is the origin of the small scale normal fluid enstrophy structures which are visible in Fig. 1.

The total energy injected into the normal fluid by the reconnection, ΔE_n, which hereafter we refer to as the energy jump, is defined as

$$\Delta E_n = \max\left[E_n(t > t_0)\right] - E_n^0, \tag{4}$$

where $E_n^0 = E_n(t_0)$ is the normal fluid kinetic energy at $t = t_0$. Normalized energy jumps are plotted in Fig. 4 as a function of the ratio A^+/A^-. Here, we observe that the larger A^+/A^- is, the smaller the normal fluid excitation is.

The emission of the sound pulse at the vortex reconnection [12] which is typical of the GPE model is absent in our incompressible hydrodynamic approach. To model this effect, the change of vortex length, ΔL, created by the vortex reconnection algorithm is always negative by construction [19], because, in the local induction approximation to the Biot-Savart law, the superfluid incompressible kinetic energy, E_s, is proportional to the vortex length, L. Such procedure ensures that at $T = 0$ K when a reconnection occurs $\Delta E_s \propto \Delta L < 0$. Consequentially, in the absence of any dissipative normal fluid, the superfluid energy E_s that would be transferred to the sound pulse, normalized with its value E_s^0 at reconnection, is $-\Delta L/L_0$., If these normalized energy jumps (black diamonds in Fig. 4) are compared to the results obtained with the compressible GPE [10] (purple squares) we find a good agreement, confirming that the model we employ, is suitable for the investigation of the feature of single reconnection events.

Implications for turbulence. — Our numerical results have implications for our understanding of quantum turbulence [27]. A fully developed turbulent tangle of vortices is characterized by its vortex line density $\mathcal{L}$ (vortex length per unit volume); the frequency of vortex reconnections per unit volume is $f = (\kappa/6\pi)\mathcal{L}^{5/2}\ln(\mathcal{L}^{-1/2}/a_0)$ [28]. From Fig. 3 we estimate the normal fluid reconnection relaxation time τ_n as the time after reconnection at which the normal fluid energy E_n/E_0 has decayed to the pre-reconnection level: in our dimensionless units, $\kappa\tau_n \approx 0.25$. Using this timescale, we estimate that the average vortex line density that is required to sustain the normal fluid in a perturbed state via frequent vortex reconnections is approximately $\mathcal{L} \approx 10^7$ to $10^8\mathrm{m}^{-2}$. Experiments in ^{4}He [29–33] and in ^{3}He [34] can achieve vortex line densities much larger than this.

Conclusions.— We have conducted an experiment using active particle tracers and a statistical numerical study of vortex reconnections in a wide range of temperatures using a model of ^{4}He which accounts for the coupled dynamics of superfluid and normal fluid components. We have verified the scaling law of the minimum vortex distance $\delta^\pm = A^\pm(\kappa|t - t_0|)^{1/2}$ and found that the approach prefactor A^- has a clear temperature dependence independent of the geometry in both experiments and numerics, in contrast to the separation prefactor A^+. The prefactors are in good agreement with GPE simulations [10, 24] and

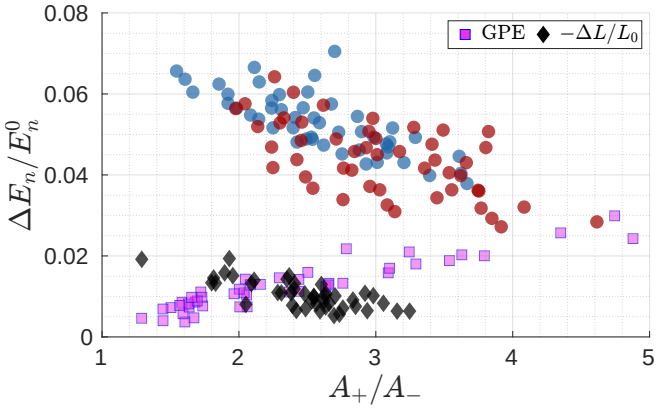

FIG. 4: Normalized energy jumps $\Delta E_n/E_n^0$ for Hopf link reconnections.The solid black diamonds are the normalized change in line length $\Delta L/L_0$ in the $T = 0$ K case. Blue and red circle correspond to $T = 1.9K$ and $T = 2.1K$,respectively. The purple squares are from GPE simulations of Villois et al. [10].

classical fluid reconnections [9] revealing that vortex reconnections display a universal behaviour regardless of the nature of the fluid (classical or quantum) and of temeperature. It is worth noting that the behaviour, as a function of A^+/A^-, of the energy injected in the normal fluid (at $T > 0$) and of the energy transferred to sound (at $T = 0$) [10, 12] is dissimilar: the former decreases as A^+/A^- increases, the latter the opposite. This likely arises from the distinct physics governing the loss of superfluid incompressible kinetic energy: mutual friction at $T > 0$, quantum pressure at $T = 0$. We have also found that a reconnection event suddenly injects an amount of energy into the normal fluid which is comparable to the energy transferred by friction during the vortex approach. Applying these results to turbulence, we have compared the decay time of the normal fluid structures created by a reconnection to the frequency of reconnections in a vortex tangle, and argued that, if the vortex line density is large enough, these punctuated energy injections should sustain the normal fluid in a perturbed state, which may lead to a new type of turbulence.

[1] J. Yao and F. Hussain, Vortex reconnection and turbulence cascade, Ann. Rev. Fluid Mech. **54**, 317 (2022).

[2] I. T. Chapman, R. Scannell, W. A. Cooper, J. P. Graves, R. J. Hastie, G. Naylor, and A. Zocco, Magnetic reconnection triggering magnetohydrodynamic instabilities during a sawtooth crash in a tokamak plasma, Phys. Rev. Lett. **105**, 255002 (2010).

[3] S. Nazarenko and R. West, Analytical solution for nonlinear Schrödinger vortex reconnection, J. Low Temp. Phys. **132**, 1 (2003).

[4] G. P. Bewley, M. S. Paoletti, K. R. Sreenivasan, and D. P. Lathrop, Characterization of reconnecting vortices in superfluid helium, Proc. Nat. Acad. Sci. USA **105**, 13707 (2008).

[5] M. S. Paoletti, M. E. Fisher, and D. P. Lathrop, Reconnection dynamics for quantized vortices, Physica D **239**, 1367 (2010).

[6] S. Zuccher, M. Caliari, A. W. Baggaley, and C. F. Barenghi, Quantum vortex reconnections, Phys. Fluids **24**, 125108 (2012).

[7] A. Villois, D. Proment, and G. Krstulovic, Universal and nonuniversal aspects of vortex reconnections in superfluids, Phys. Rev. Fluids **2**, 044701 (2017).

[8] L. Galantucci, A. W. Baggaley, N. G. Parker, and C. F. Barenghi, Crossover from interaction to driven regimes in quantum vortex reconnections, Proc. Nat. Acad. Sci. USA **116**, 12204 (2019).

[9] J. Yao and F. Hussain, Separation scaling for viscous vortex reconnection, J. Fluid Mech. **900**, R4 (2020).

[10] A. Villois, D. Proment, and G. Krstulovic, Irreversible dynamics of vortex reconnections in quantum fluids, Phys. Rev. Lett. **125**, 164501 (2020).

[11] D. Proment and G. Krstulovic, Matching theory to characterize sound smission during vortex reconnection in quantum fluids, Phys. Rev. Fluids **5**, 104701 (2020).

[12] M. Leadbeater, T. Winiecki, D. C. Samuels, C. F. Barenghi, and C. S. Adams, Sound emission due to superfluid vortex reconnections, Phys. Rev. Lett. **86**, 1410 (2001).

[13] M. S. Paoletti, M. E. Fisher, K. R. Sreenivasan, and D. P. Lathrop, Velocity statistics distinguish quantum turbulence from classical turbulence, Physical review letters **101**, 154501 (2008).

[14] W. Guo, M. La Mantia, D. P. Lathrop, and S. W. Van Sciver, Visualization of two-fluid flows of superfluid helium-4, Proceedings of the National Academy of Sciences **111**, 4653 (2014).

[15] C. Peretti, J. Vessaire, Émeric Durozoy, and M. Gibert, Direct visualization of the quantum vortex lattice structure, oscillations, and destabilization in rotating ¡sup¿4¡/sup¿he, Science Advances **9**, eadh2899 (2023), https://www.science.org/doi/pdf/10.1126/sciadv.adh2899.

[16] U. Giuriato and G. Krstulovic, Quantum vortex reconnections mediated by trapped particles, Phys. Rev. B **102**, 094508 (2020).

[17] KW. Schwarz, Three-dimensional vortex dynamics in superfluid ^{4}He, Phys. Rev. B **38**, 2398 (1988).

[18] L. Galantucci, A. W. Baggaley, C. F. Barenghi, and G. Krstulovic, A new self-consistent approach of quantum turbulence in superfluid helium, Eur. Phys. J. Plus **135**, 547 (2020).

[19] A. W. Baggaley, The sensitivity of the vortex filament method to different reconnection models, J. Low Temp. Phys. **168**, 18 (2012).

[20] See Supplementary Material.

[21] D. Kivotides, C. F. Barenghi, and D. C. Samuels, Triple vortex ring structure in superfluid helium ii, Science **290**, 777 (2000).

[22] L. Boué, D. Khomenko, V. L'vov, and I. Procaccia, Analytic solution of the approach of quantum vortices towards reconnection, Phys. Rev. Lett. **111**, 145302 (2013).

[23] R. S, Self-similar vortex reconnection, C. R. Méc **347**, 365 (2019).
[24] A. J. Allen, S. Zuccher, M. Caliari, N. P. Proukakis, N. G. Parker, and C. F. Barenghi, Vortex reconnections in atomic condensates at finite temperature, Phys. Rev. A **90**, 013601 (2014).
[25] L. Galantucci, G. Krstulovic, and C. Barenghi, Friction-enhanced lifetime of bundled quantum vortices, Phys. Rev. Fluids **8**, 014702 (2023).
[26] P. Z. Stasiak, A. W. Baggaley, G. Krstulovic, C. F. Barenghi, and L. Galantucci, Cross-component energy transfer in superfluid helium-4, J. Low Temp. Phys. (2024).
[27] C. F. Barenghi, L. Skrbek, and K. R. Sreenivasan, *Quantum Turbulence* (Cambridge University Press, 2023).
[28] C. F. Barenghi and D. C. Samuels, Scaling laws of vortex reconnections, J. Low Temp. Phys. **136**, 281 (2004).
[29] K. W. Schwarz and C. W. Smith, Pulsed-ion study of ultrasonically generated turbulence in superfluid 4He, Physics Letters A **82**, 251 (1981).
[30] F. P. Milliken, K. W. Schwarz, and C. W. Smith, Free Decay of Superfluid Turbulence, Phys. Rev. Lett. **48**, 1204 (1982).
[31] P.-E. Roche and C. F. Barenghi, Vortex spectrum in superfluid turbulence: Interpretation of a recent experiment, EPL **81**, 36002 (2008).
[32] P.-E. Roche, P. Diribarne, T. Didelot, O. Français, L. Rousseau, and H. Willaime, Vortex density spectrum of quantum turbulence, EPL **77**, 66002 (2007).
[33] S. Babuin, E. Varga, L. Skrbek, E. Lévêque, and P.-E. Roche, Effective viscosity in quantum turbulence: a steady state approach, Europhys. Lett. **106**, 24006 (2014).
[34] D. I. Bradley, D. O. Clubb, S. N. Fisher, A. M. Guénault, R. P. Haley, C. J. Matthews, G. R. Pickett, V. Tsepelin, and K. Zaki, Decay of pure quantum turbulence in superfluid ^{3}He-B, Phys. Rev. Lett. **96**, 035301 (2006).